Engineering of fast mode conversion in multimode waveguides

Shuo-Yen Tseng[1,2,*] and Xi Chen[3,4,5]

[1]*Department of Photonics, National Cheng Kung University, Tainan 701, Taiwan*

[2]*Advanced Optoelectronic Technology Center, National Cheng Kung University, Tainan 701, Taiwan*

[3]*Department of Physics, Shanghai University, Shanghai 200444, China*

[4]*Departamento de Química Física, UPV-EHU, Apdo 644, Bilbao E-48080, Spain*

[5]*e-mail: xchen@shu.edu.cn*

**Corresponding author: tsengsy@mail.ncku.edu.tw*

Received October 26, 2012; revised November 9, 2012; accepted November 13, 2012; posted November 13, 2012 (Doc. ID 178785); published December 7, 2012

We propose fast and robust mode conversion in multimode waveguides based on Lewis–Riesenfeld invariant theory. The design of mode converters using the multimode driving for dynamical invariant is discussed. Computer-generated planar holograms are used to mimic the shaped pulses driving the states in three-level quantum systems. We show that the invariant-based inverse engineering scheme reduces mode converter length as compared to the common adiabatic scheme. © 2012 Optical Society of America

OCIS codes: 130.3120, 130.2790, 090.1760, 000.1600.

Mode-division multiplexing (MDM) is a promising technique where multiple optical modes are used as independent data channels to transmit optical data [1]. One important building block for MDM systems is the mode converter [2,3]. The two major routes to realize mode conversion in integrated optics devices are resonant coupling and adiabatic coupling. Resonant devices can be made very short but are highly sensitive to fabrication variations, whereas adiabatic coupling devices are robust against fabrication imperfections but long. A similar problem in atomic and molecular physics is the control of system state population by laser pulses [4]. Resonant pulse provides fast population transfer but is not robust, whereas adiabatic passage techniques are too slow. To combine the advantages of both resonant and adiabatic techniques, several schemes have been proposed [5–9], where specially shaped pulses are used to achieve fast and high-fidelity state control. Recently, analogies between quantum mechanics and wave optics in integrated optics devices have been exploited to realize many interesting devices [10–12]. The similarities allow a straightforward adaptation of schemes developed for quantum system manipulation to the design of waveguide based devices. We have previously proposed adiabatic mode conversion devices using computer-generated planar holograms (CGPHs) [13] in multimode waveguides based on stimulated Raman adiabatic passage (STIRAP) [14] in a three-level system. Figure 1 shows a three-level system and the schematic of a corresponding CGPH loaded multimode waveguide, where multiplexed long-period gratings with coupling coefficient variations along the propagation direction are used to mimic the delayed laser pulses in STIRAP. Recently, we demonstrated a shortcut to STIRAP mode conversion [15] based on transitionless quantum driving [7,8]. In this Letter, we use invariant-based inverse engineering [16] to realize a fast and robust shortcut to mode conversion without the need of direct coupling of modes $|\Psi_1\rangle$ and $|\Psi_3\rangle$.

For a quantum system evolving with a time-dependent Hamiltonian $\mathbf{H}(t)$, the corresponding Schrödinger equation is $i\hbar\partial_t|\Psi(t)\rangle = \mathbf{H}(t)|\Psi(t)\rangle$. An invariant $\mathbf{I}(t)$, which satisfies $\partial\mathbf{I}/\partial t + (1/i\hbar)[\mathbf{I},\mathbf{H}] = 0$, gives the relation, $i\hbar\partial_t(\mathbf{I}(t)|\Psi(t)\rangle) = \mathbf{H}(t)(\mathbf{I}(t)|\Psi(t)\rangle)$ [17]. That is, acting on a solution of the Schrödinger equation, the invariant produces another solution of the Schrödinger equation. The result implies that an arbitrary solution of the Schrödinger equation can be written as a superposition of the eigenstates $\phi_n(t)$ of the invariant $\mathbf{I}(t)$. According to Lewis–Riesenfeld theory, we can write $\Psi(t) = \sum_n c_n e^{i\alpha_n}\phi_n(t)$, where α_n is the Lewis–Riesenfeld phase, and c_n is a time-*independent* amplitude [17]. The time-independent c_n's allow the engineering of the evolution of $\Psi(t)$ using $\phi_n(t)$ without worrying about the coupling among them.

In a step-index multimode waveguide supporting $N \geq 3$ forward-propagating modes, we consider three distinct modes $|\Psi_1\rangle$, $|\Psi_2\rangle$, and $|\Psi_3\rangle$, coupled by a CGPH. We can design the CGPH to mimic the STIRAP process, so the evolution of mode amplitudes $A_i(i = 1,2,3)$ obey the coupled mode equations, $i(\partial/\partial z)\mathbf{A} = \mathbf{H}(z)\mathbf{A}$, where $\mathbf{A} = [A_1, A_2, A_3]^T$, and the matrix element κ_{ij} of $\mathbf{H}$ denotes the coupling coefficients between $|\Psi_i\rangle$ and $|\Psi_j\rangle$. Replacing the spatial variation z with the temporal variation t, the same equations can be used to describe the probability amplitudes of a three-level atomic system driven by two laser pulses using the Schrödinger equation ($\hbar = 1$). The associated Hamiltonian (where t is replaced by z and hereafter) is

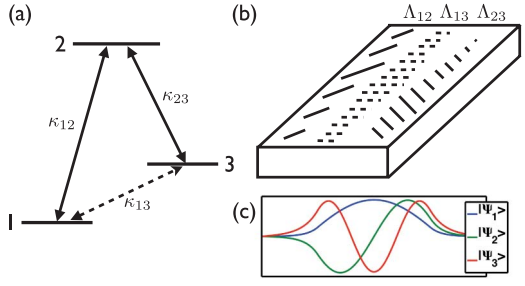

Fig. 1. (Color online) (a) Level scheme of a three-level Λ system. (b) Schematic of a CGPH loaded multimode waveguide. (c) Amplitude profiles of the three guided modes.

$$\mathbf{H}(z) = \frac{\hbar}{2}\begin{bmatrix} 0 & \kappa_{12}(z) & 0 \\ \kappa_{21}(z) & 0 & \kappa_{23}(z) \\ 0 & \kappa_{32}(z) & 0 \end{bmatrix}. \quad (1)$$

Solving for the eigenmodes $|\Psi_D\rangle$, $|\Psi_+\rangle$, and $|\Psi_-\rangle$, we obtain $|\Psi_D\rangle = [\cos\theta, 0, \sin\theta]^T$, where $\tan\theta = \kappa_{12}/\kappa_{23}$. When the adiabatic condition $|\partial\theta/\partial z| \equiv |\dot{\theta}| \ll |\sqrt{\kappa_{12}^2 + \kappa_{23}^2}|$ is satisfied and the coupling coefficients $\kappa_{12}(z)$ and $\kappa_{23}(z)$ are applied in a counterintuitive scheme as in STIRAP, $|\Psi_D\rangle$ can be used to convert $|\Psi_1\rangle$ to $|\Psi_3\rangle$ adiabatically. We can speed up the transfer using the invariant-based shortcut. The Hamiltonian in Eq. 1 possesses SU(2) symmetry, and an invariant $\mathbf{I}(t)$ is given by [18]

$$\mathbf{I}(z) = \frac{\hbar}{2}\begin{bmatrix} 0 & \cos\gamma\sin\beta & -i\sin\gamma \\ \cos\gamma\sin\beta & 0 & \cos\gamma\cos\beta \\ i\sin\gamma & \cos\gamma\cos\beta & 0 \end{bmatrix} \quad (2)$$

with

$$\kappa_{12} = 2(\dot{\beta}\cot\gamma\sin\beta + \dot{\gamma}\cos\beta), \quad (3)$$

$$\kappa_{23} = 2(\dot{\beta}\cot\gamma\cos\beta - \dot{\gamma}\sin\beta). \quad (4)$$

The eigenmodes of $\mathbf{I}(z)$ are

$$|\phi_0\rangle = \begin{bmatrix} \cos\gamma\cos\beta \\ -i\sin\gamma \\ -\cos\gamma\sin\beta \end{bmatrix}, \quad (5)$$

$$|\phi_\pm\rangle = \frac{1}{\sqrt{2}}\begin{bmatrix} \sin\gamma\cos\beta \pm i\sin\beta \\ i\cos\gamma \\ -\sin\gamma\sin\beta \pm i\cos\beta \end{bmatrix}. \quad (6)$$

To convert $|\Psi_1\rangle$ to $|\Psi_3\rangle$ in an arbitrarily short device length L, we choose $\gamma(z) = \epsilon$ and $\beta(z) = \pi z/2L$ in Eqs. (3) and (4) to obtain [18]

$$\kappa_{12} = (\pi/L)\cot\epsilon\,\sin(\pi z/2L), \quad (7)$$

$$\kappa_{23} = (\pi/L)\cot\epsilon\,\cos(\pi z/2L). \quad (8)$$

By choosing ϵ as the solution of $\sin^{-1}\epsilon = 4N, (N = 1, 2, 3\ldots)$ (multimode driving scheme) [18], the superposition of $|\phi_0(0)\rangle$ and $|\phi_\pm(0)\rangle$ corresponds to $|\Psi_1\rangle$, and the superposition of $|\phi_0(L)\rangle$ and $|\phi_\pm(L)\rangle$ corresponds to $|\Psi_3\rangle$, so that the light evolution will follow the eigenmodes of the invariant and converts $|\Psi_1\rangle$ to $|\Psi_3\rangle$. In the following numerical example, we design CGPHs to implement the coupling coefficients Eqs. (7) and (8) to demonstrate mode conversion using the multimode driving scheme.

We consider a 3 μm wide, five-moded polymer waveguide similar to the one in [15] for mode conversion from $|\Psi_1\rangle$ to $|\Psi_3\rangle$. The CGPH is designed at the zero-detuning wavelength $\lambda_0 = 1.55$ μm and the TE polarization. The maximum effective index modulation is assumed to be $\Delta n = 0.003$. We simulate a mode converter at 4 mm length using the beam propagation method (BPM). The coupling coefficients κ_{12} and κ_{23} are calculated using Eqs. (7) and (8) with $\epsilon = 0.2527$, and the calculated k_{12} and k_{23} are directly proportional to Δn in the waveguide. The designed CGPH to implement the coupling matrix Eq. (1) is shown in Fig. 2. The CGPH pattern is used as an effective index perturbation to the multimode waveguide. Figure 3 shows the calculated beam propagation in the mode converter using mode $|\Psi_1\rangle$ as the input from the left hand side. According to the multimode driving scheme, $|\Psi_1\rangle$ is converted to $|\Psi_3\rangle$ at the output on the right hand side in a 4 mm device. In Fig. 4, the corresponding modal power evolution along the propagation distance is shown, and the result agrees with theoretical predictions in [18]. The smooth conversion curve shows the good device length tolerance, which is characteristic of adiabatic devices. Clearly, the invariant-based

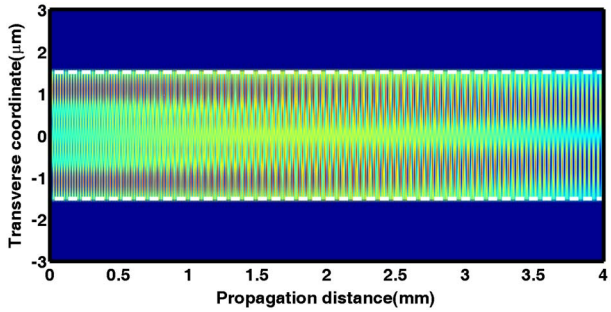

Fig. 2. (Color online) Calculated CGPH pattern for mode conversion. Dashed lines indicate the waveguide core.

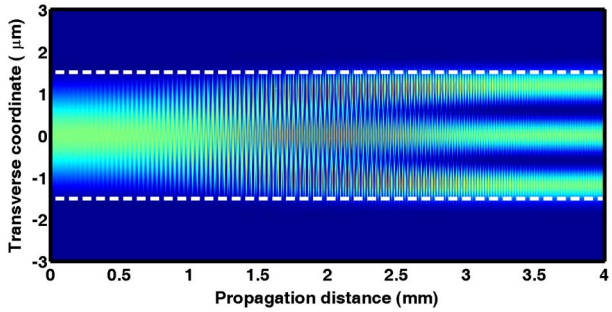

Fig. 3. (Color online) BPM simulation of light propagation in a 4 mm mode converter based on the multimode driving scheme. Dashed lines indicate the waveguide core.

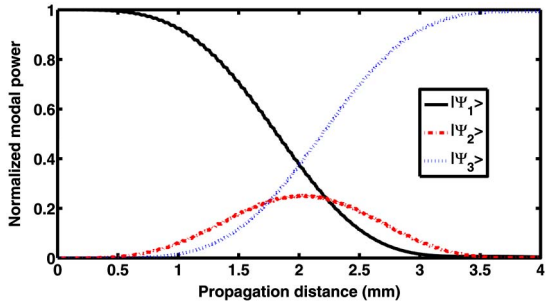

Fig. 4. (Color online) Modal power evolution in a 4 mm mode converter using the multimode driving scheme.

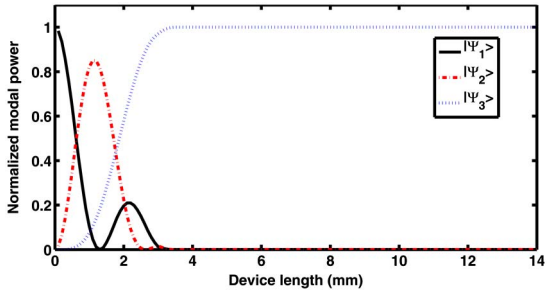

Fig. 5. (Color online) Normalized modal power at the mode converter output for different device lengths.

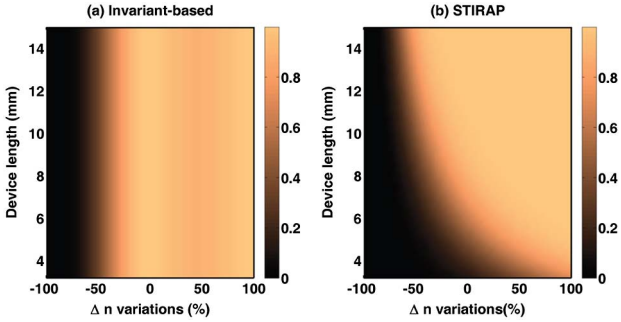

Fig. 6. (Color online) Normalized output power in $|\Psi_3\rangle$ against Δn variations ($\Delta n = 0.003$ at 0%). (a) Invariant-based and (b) STIRAP.

multimode driving scheme can be realized in an engineered multimode waveguide.

Next, we calculate the shortest converter length using the multimode driving scheme. We numerically solve the coupled mode equations using κ_{12} and κ_{23} defined in Eqs. (7) and (8) with $\epsilon = 0.2527$ and plot the normalized modal power at the output of the converter as a function of the device length in Fig. 5. We note that the maximum value of coupling coefficient corresponding to $\Delta n = 0.003$ is 2.022 mm^{-1} for κ_{12} and 1.755 mm^{-1} for κ_{23} in this polymer waveguide platform in our numerical example. So, we cap the maxima of κ_{12} and κ_{23} at 2.022 mm^{-1} and 1.755 mm^{-1}, respectively, in our simulation to account for physical realizability in fabrication and to avoid additional scattering loss resulting from large effective index modulation. To obtain a conversion efficiency ≥99%, the device length can be reduced to 3.2 mm in this numerical example, compared to 11.4 mm in the conventional STIRAP converter [15]. The invariant-based scheme fails at lengths below 3.2 mm because of the limitation we put on the maximum value of κ_{12} and κ_{23}. Next, we investigate the device performance against fabrication variations. Errors in the CGPH etch depth is directly related to Δn, which in turn affects the coupling coefficients proportionally. In Fig. 6(a), we plot the normalized modal power of $|\Psi_3\rangle$ at the output for different device lengths with Δn variations. The case for conventional STIRAP converters is shown in Fig. 6(b). The robustness of the invariant-based device is comparable to that of sufficiently long (≥11.4 mm) STIRAP devices. We also note that there are several possibilities on designing the coupling coefficients, and one can further combine the optimal control method to optimize the device performance in regard to robustness against Δn variations [18].

In summary, invariant-based inverse engineering of fast and robust mode conversion in multimode waveguides is investigated. The multimode driving scheme, originally developed to speed up population transfer in three-level quantum systems, can be readily applied to the design of integrated optical mode converters.

We thank J. Gonzalo Muga for his comments and discussions. S.-Y. T's work is supported by the National Science Council of Taiwan under contract NSC 100-2221-E-006-176-MY3. X. C. acknowledges support from National Natural Science Foundation of China (Grant No. 61176118), Shanghai Rising-Star Program (Grant No. 12QH1400800), Basque government (Grant No. IT472-10), Ministerio de Ciencia e Innovacion (Grant No. FIS2009-12773-C02-01), and the UPV/EHU under program UFI 11/55.

References

1. S. Berdagué and P. Facq, Appl. Opt. **21**, 1950 (1982).
2. A. Fratalocchi, R. Asquini, and G. Assanto, Opt. Express **13**, 32 (2005).
3. A. Fratalocchi and G. Assanto, Appl. Phys. Lett. **86**, 051109 (2005).
4. K. Bergmann, H. Theuer, and B. W. Shore, Rev. Mod. Phys. **70**, 1003 (1998).
5. G. S. Vasilev, A. Kuhn, and N. V. Vitanov, Phys. Rev. A **80**, 013417 (2009).
6. G. Dridi, S. Guérin, V. Hakobyan, H. R. Jauslin, and E. Eleuch, Phys. Rev. A **80**, 043408 (2009).
7. X. Chen, I. Lizuain, A. Ruschhaupt, D. Guéry-Odelin, and J. G. Muga, Phys. Rev. Lett. **105**, 123003 (2010).
8. M. V. Berry, J. Phys. A: Math. Theor. **42**, 365303 (2009).
9. X. Chen, A. Ruschhaupt, S. Schmidt, A. del Campo, D. Guéry-Odelin, and J. G. Muga, Phys. Rev. Lett. **104**, 063002 (2010).
10. S. Longhi, Laser Photon. Rev. **3**, 243 (2009).
11. E. Paspalakis, Opt. Commun. **258**, 30 (2006).
12. A. A. Rangelov and N. V. Vitanov, Phys. Rev. A **85**, 055803 (2012).
13. S.-Y. Tseng, Y. Kim, C. J. K. Richardson, and J. Goldhar, Appl. Opt. **45**, 4864 (2006).
14. S.-Y. Tseng and M.-C. Wu, IEEE Photon. Technol. Lett. **22**, 1211 (2010).
15. T.-Y. Lin, F.-C. Hsiao, Y.-W. Jhang, C. Hu, and S.-Y. Tseng, Opt. Express **20**, 24085 (2012).
16. X. Chen, E. Torrontegui, and J. G. Muga, Phys. Rev. A **83**, 062116 (2011).
17. H. R. Lewis and W. B. Riesenfeld, J. Math. Phys. **10**, 1458 (1969).
18. X. Chen and J. G. Muga, Phys. Rev. A **86**, 033405 (2012).